Research Square

Preprints are preliminary reports that have not undergone peer review.
They should not be considered conclusive, used to inform clinical practice,
or referenced by the media as validated information.

Lignin nanoparticles for sustainable and biodegradable packaging films

Bongkot Hararak (bongkoth@mtec.or.th)
Metal and Materials Technology Center
Charinee Winotapun
Metal and Materials Technology Center
Natcha Prakymoramas
Metal and Materials Technology Center
Wattana Klinsukhon
Metal and Materials Technology Center
Pawarisa Wijaranakul
Metal and Materials Technology Center

Research Article

Keywords: Lignocellulosic material, Lignin nanoparticles, Bio-based, Films, Functional, Composites

Posted Date: March 23rd, 2022

DOI: https://doi.org/10.21203/rs.3.rs-1456679/v1

License: This work is licensed under a Creative Commons Attribution 4.0 International License.
Read Full License

Abstract

A simple, green, and scalable procedure to manufacture spherical lignin nanoparticles is demonstrated in this work. Softwood kraft lignin (S-lignin) was fractionated using acetone which was recoverable and reused in the following step to produce lignin nanoparticles (S-LNPs). Deionized water was used as anti-solvent to precipitate S-LNPs under ultrasonication. The size of S-LNPs was found to be in the range from 40-300 nm with an average of 120±18 nm. S-LNPs had lower ash content at 0.05% as compared to 1.22% of S-lignin. More importantly, S-LNPs had significant increased phenolic to aliphatic hydroxyl ratio. Home-composable polybutylene succinate (PBS) was selected to develop sustainable materials for flexible film applications. Composite films of PBS/S-lignin and PBS/S-LNPs were manufactured via conventional blown film melt-extrusion. Both composite films appeared brownish. At 0.5 wt% loading content, the PBS/S-LNPs composite films possessed comparable mechanical properties to the neat PBS film with several advantages including (a) a superb UV-blocking ability of 69% and 64% enhancement in shielding of UV-B and UV-A, respectively; (b) retardation of thermo-oxidative reaction with 42 % improvement in onset oxidative temperature; and (c) antibacterial activity (R) values of 2.5 for gram-negative (*E. coli* ATCC8739) and 1.5 for gram-positive (*S. aureus* ATCC 6538p). For a meaningful approach in fully biodegradable and sustainable plastic products, the spherical lignin nanoparticles produced in this work can be alternative multifunctional bio-additives for UV protection, antioxidation and antibacterial applications.

1. Introduction

There is no doubt that usage and waste management of synthetic plastics have been reshaping. 170 million tons of plastic food packaging represent the largest end-used market which contributing close to 40% of the overall demand of synthetic plastics [1, 2]. Large quantity of plastic waste and mismanagement cause serious deteriorations of ecological environment and human health. Plastic wastes have been discarded in landfilled and marine and have caused many concerns. Mega and macro-scale plastic wastes are harmful for animals from eating and getting stuck [3]. Moreover, these plastic wastes can be further fragmented into small debris, known as microplastics, which become a source of air pollution as airborne fibrous particles suspended in air [4]. Furthermore, they have been found in the digestive tracts and tissues of various sea animals [5]. From waste management point of view, classification and management of recyclable post-consumer plastics have not been achieved in every country [6]. Due to the overall concerns, there is a need for materials that are biodegradable and eco-friendly plastics to mitigate plastic waste problems.

Several alternative biodegradable plastics have been introduced in both academic and industrial fields toward for sustainable world. Biobased and biodegradable resins such as starch blend, polylactic acid (PLA), polybutylene succinate (PBS) and polyhydroxybutyrate (PHB), and petroleum-based biodegradable resins including polybutylene adipate-co-terephthalate (PBAT), and polycaprolactone (PCL) are commercially available for industrial plastic fabrications through conventional extrusion and injection processes [7]. All those biodegradable plastics are expected to substituent some applications of non-

biodegradable plastic such single-used plastics, medical plastics and contaminated packaging applications in sustainable future. PBS can be one of the promising material choices for replacing single-used plastic because it is a home-compostable plastic [6, 8]. Moreover, its thermal stability, processability and excellent mechanical properties are comparable with isotactic polypropylene (PP). However, PBS has high light transmittance and high resin cost. These may be barriers for both technical and market feasibilities. Therefore, reducing its cost and enhancing the light barrier have been required as viable issues. Adding inexpensive fillers into PBS is one of the practical solutions to lower the price of PBS products [9–11]. Selection of bio-renewable and biodegradable fillers becomes a promising choice to maintain the composite biodegradability and lower the PBS cost. Thus, fillers from biomass resources such as plant fibers, agricultural residues and lignocellulosic materials (cellulose, hemicellulose and lignin) are highly recommended.

Lignin is the most abundant and renewable aromatic biopolymer on earth [12]. Over 55% of technical lignin, about 81 million tons annually, is obtained from pulping industries where a kraft process is used [13]. High value-added application of lignin is very limited due to its complex structure with three-dimensional network interacting with carbohydrate causing a difficulty to be isolated and purified [14, 15]. Most technical lignins have an irregular shape, large particle sizes in a range of few microns to 100 μm and a broad particle size distribution [16]. Lignin offers numerous unique features such as high carbon content [17], high thermal stability [18], superb UV-shielding ability [8, 19], and antimicrobial and antioxidant properties [20, 21]. Such attractive features as well as its low cost, renewability and biodegradability have promoted lignin to be an interesting material for sustainable products. Up to now, micro-scale lignin has been recognized as a low-cost filler, used as fire retardant, antimicrobial, antioxidant, and blocking of ultraviolet (UV) irradiation. Domínguez-Robles *et al.* [22] had introduced up to 15 wt% of micro-scale lignin in PBS via melt extrusion and injection molded processes. The resultant PBS/lignin composites revealed a capability to be a radical scavenger and resistance to adherence of the common nosocomial pathogen, *Staphylococcus aureus*, whereas the mechanical properties (tensile, flexural and impact) significant decreased. Similar trend of decreasing mechanical properties has been reported in other polymers [19, 23–26]. This may be due to large lignin particles having low surface area, high agglomeration and poor interaction with the host polymers [27, 28]. Chemical modification of lignin has been reported to enhance its compatibility with the host polymers [8, 29, 30]. Moreover, use of such large lignin particles might not be suitable for applications of flexible film with a thickness of 10–60 μm [31, 32]. One of the alternative methods is synthesizing lignin nanoparticles (LNPs) [33–36]. LNPs offers several advantages due to their large surface area, resulting in improved properties of final products and compatibility to host polymers [34, 36]. It was reported that nanocomposite LNPs films could be formed by either solution casting [8, 19, 37–39] or melt-extrusion process [40]. For industrial production aspect, melt-extrusion process is preferred for preparing flexible films for food packaging in order to accomplish economical and practical key points.

Herein, we developed sustainable films from PBS and LNPs using a simple and green approach to purify lignin from kraft process. Small amount of LNPs (0.1-1.0 wt%) without any chemical modification was incorporated into PBS via melt extrusion and the nanocomposite films of PBS/LNPs were formed by

blown film extrusion process. Properties of resultant nanocomposite films including physical appearance, film color, thermal and mechanical properties are reported and discussed. Furthermore, the PBS/LNPs nanocomposite films showed excellent active functions of UV-blocking, antioxidation and antibacterial, which indicated promising applications in various practical fields.

2. Materials And Method

2.1 Materials

Softwood kraft lignin, BioPivaTM100, was purchased from UPM Biochemicals, Finland. In this work softwood kraft lignin was coded as S-lignin. Commercially available biodegradable polybutylene succinate (PBS), FZ91 PM, was purchased from PPT Global Chemical Public Company Limited, Thailand. Anhydrous pyridine, deuterated chloroform ($CDCl_3$), endo-N-hydroxy-5-norbornene-2,3-dicarboximide (NHND), 2-chloro-4,4,5,5-tetramethyl1,3,2-dioxaphospholane (TMDP), chromium (III) acetylacetonate were purchased from Sigma-Aldrich, Singapore.

2.2 Preparation of lignin nanoparticles (S-LNPs)

2.2.1 Purification of S-lignin by fractionation using acetone

S-lignin was pre-dried in a vacuum oven for 6 hours prior to fractionation using acetone. 10 g of the pre-dried S-lignin was placed in a three-neck flask containing 100 ml of acetone. The top-neck of flask was attached to a water condenser, whilst other two necks were attached to a thermocouple and nitrogen bubbling at a flow rate of 10 ml/minute. The flask was placed on a heating mantle with magnetic stirrer and the lignin solution was stirred for 6 hours at 56 °C. Acetone-soluble fraction was then filtrated through a 1 µm glass filter, and remaining acetone was evaporated using rotary evaporator with water bath at 40 °C. The obtained acetone-soluble lignin was dried at 80 °C in a vacuum oven and ground into powders. Ash content of acetone-soluble lignin was determined in a comparison with the pristine S-lignin.

2.2.2 Production of S-LNPs

1 g of acetone-soluble lignin was dissolved in 20 ml acetone at room temperature. After lignin was fully dissolved, 20 ml of acetone-soluble lignin solution was poured into 200 ml deionized water at room temperature under ultrasonication (VCX 500 sonicator, 500-watt, 20 kHz and 13 mm probe) for 5 minutes. Figure 1 illustrates a protocol used for the preparation of S-LNPs from S-lignin. S-LNPs was obtained after centrifugation at 10000 rpm for 20 minutes and then dried in a vacuum oven at 80 °C for 6 hours.

2.3 Preparation of PBS composite films

In this work, 2 types of lignin (S-lignin and S-LNPs) were used to prepare PBS/lignin composite films. 2 g of lignin was pre-mixed with 98 g of PBS to obtain 2 wt% PBS/lignin compound. The pre-mixed was loaded into co-rotating twin screw extruder (Thermo Scientific Process 11, 11-mm screw diameter and a ratio of screw length to diameter (L/D) of 40). Barrel temperature profile was set at 140 °C, 140 °C, 150 °C,

155 °C, 160 °C, 160 °C and 160 °C and die temperature was at 155 °C. The PBS/lignin compounds were extruded through 3-mm die diameter with 45 rpm screw speed, the brownish extrudate was air-cooled prior to pelletizing. The obtained 2 wt% PBS/lignin compounds were kept in an airtight container until used.

PBS composite films at different lignin contents of 0.1, 0.2, 0.5 and 1.0 wt% were prepared via single screw extruder (PolyLab™, HAAKE). A standard metering screw (3:1) with 19-mm diameter and L/D of 25 was equipped with a blown film die with 35 mm outer diameter and 1 mm die gap. Temperatures of three heating zones and die were 150, 155, 160 °C and 160 °C, respectively. To prepare composite films at the controlled thickness of 35 µm and 13-cm width. Screw speed, blow-up ratio (BUR) and take up speed were 60 rpm, 2.75 and 3.7 m/minute, respectively. Neat PBS film and PBS/S-LNPs composite films at 0.1, 0.2, 0.5 and 1.0 wt% were named as neat PBS, PBS/S-LNPs_0.1, PBS/S-LNPs_0.2, PBS/S-LNPs_0.5 and PBS/S-LNPs_1.0, respectively. PBS/S-lignin composite films at the same aforesaid contents were prepared for comparison.

2.4 Characterizations

Ash content of lignin samples (S-lignin and S-LNPs) was determined in accordance with TAPPI T211 om-02 method by combustion at 525°C using a muffle furnace (Carbolite model RHF16).

A field emission scanning electron microscope (FE-SEM, model SU5000, Hitachi, Japan) was used to examine morphology of S-lignin and S-LNPs. The samples were coated with platinum for 60 seconds by Quorum-Q150RS (UK), a distance between target and the sample surface was 3 cm and the applied current of 15 mA. FE-SEM was operated at an accelerating voltage between 3 to 5 kV.

Particle size and particle size distribution of S-LNPs were examined using dynamic light scattering (DLS) technique at 25°C with Malvern Zetasizer-4 instrument (UK). Dispersion of S-LNPs was loaded into a cuvette of 1-cm path length. Three measurements were conducted and each measurement was run in triplicate. Average particles size diameter and particle size distribution index or polydispersity index (PdI) *of S-LNPs were reported.*

Glass transition temperature (T_g) of S-lignin and S-LNPs was measured using differential scanning calorimeter (DSC, model TGA/DSC3+, Mettler Toledo, Switzerland). Approximate 5 mg of pre-dried lignin samples were placed in 40 µl aluminium pans. In the first scan, the lignin samples were heated from 25°C to 105°C at a heating rate of 10°C/minute and kept isothermal for 5 minutes to remove moisture. Then, the samples were cooled to 25°C at the cooling rate of 10°C/minute and held for 3 minutes. The second heating scans was conducted from 25°C to 200°C with a heating rate of 10°C/minute. All of the scans were conducted under nitrogen atmosphere at a flow rate of 20 ml/minute.

Phosphorus-31 nuclear magnetic resonance spectroscopy (^{31}P NMR) was conducted to determine molecular structures and quantitative analysis was carried out using AV-500 Bruker Biospin NMR spectrometer. Protocol of ^{31}P NMR solution preparation was followed steps reported in Nature protocol

[41]. NHND was used as internal standard. Briefly, anhydrous pyridine/$CDCl_3$ (1.6:1 v/v) was prepared as solvent mixture A. 5 mg of chromium (III) acetylacetonate and 18 mg of NHND were mixed with 1 ml of the solvent mixture A and used as an internal standard (IS) solution. 0.1 ml of IS solution was loaded into 4-ml glass vial; the actual weight of the 0.1 ml solution was recorded. 30 mg of pre-dried lignin sample and 0.5 ml of solvent mixture A were mixed, and the solution was stirred overnight to fully dissolve the lignin samples. Finally, 0.1 ml phosphitylation reagent TMDP was added into the vial and stirred for 2 minutes. Then, all the phosphitylated lignin solution was transferred into a 5 mm NMR tube for subsequent ^{31}P NMR acquisitions (298 K, 500 MHz, 256 scans with 5s relaxation delay time using an inverse-gated decoupling pulse sequence). The obtained spectra were processed and analyzed using Bruker Topspin software.

Datacolor spectrophotometer (Spectro 650, Pakisatan) was conducted for measuring *color and opacity of the neat PBS and its composite films.* Chromatic coordinates including L*, a*, b* of CIELAB color system of neat PBS films were recorded. ΔL*, Δa*, and Δ b* of PBS/lignin composite films were reported based on the neat PBS. Color difference (ΔE) was used to indicate color change of PBS films upon addition of S-lignin and S-LNPs. ΔE was calculated using Eq. (1) [20, 42].

$$\Delta E = \sqrt{\left(L^*\right)^2 + \left(a^*\right)^2 + \left(b^*\right)^2} \quad (1)$$

Thermal characteristics of the neat PBS and its composite films were determined using differential scanning calorimeter (DSC, model TGA/DSC3+, Mettler Toledo, Switzerland). 5–7 mg of film samples were cut and placed in 40 µl-aluminum pans. The first heating scan was conducted from 40 °C to 150 °C at 10 °C/minute. Then, the sample was cooled at cooling rate of 10 °C/minute to 40 °C and reheated to 150 °C at 10 °C/minute for the second heating scan. From DSC thermogram, percentage (%) of crystallinity (X_c) was calculated using the following equation [20]:

$$X_c(\%) = \frac{\Delta H_f}{W \bullet \Delta H_f^0} \times 100 \quad (2)$$

where ΔH_f is heat of fusion of sample obtained from the second heating scan. W is weight fraction of PBS in the composite films. ΔH_f^0 is heat of 100% crystalline PBS which is 200 J/g [10, 43].

Mechanical properties of the neat PBS film and PBS/lignin composite films were determined using a universal testing machine (Instron 44502 series, Instron, USA), according to ASTM D882. Film samples were cut into 50 mm gauge length along two direction of machine direction (MD) and transvers direction (TD) at 15 mm width. The samples were tested with a crosshead speed of 100 mm/minute. At least 5 samples were tested and averaged values were reported.

UV shielding performance of PBS/lignin composite films was conducted and compared with the neat PBS film using UV–VIS spectrophotometer (UV-3600Plus, Shimadzu, Japan). Transmittance of UVA (320 to 400 nm) and UVB (290 to 320 nm) was calculated using Eq. (3), where $T()$ is spectra transmittance in percentage of each measured wavelength [44].

$$Average\ transmission\ (\%) = \sum_{\lambda_{Initial}}^{\lambda_{End}} T(\lambda)/n \qquad (3)$$

Oxidation induction temperature (OIT_{temp}) of the resultant composite films was determined using DSC (model TGA/DSC3+, Mettler Toledo, Switzerland) and the following protocol. Approximate 5 mg of the films was placed in 40 µl-aluminum pan without lid. All samples were heated from 40 to 105 °C at a rate of 10 °C/minute and kept isothermally at 105 °C for 20 minutes prior to quenched to 40 °C at a rate of 20 °C/minute and isothermally condition at 40°C for 5 minutes under nitrogen atmosphere. Finally, the samples were heated at a rate of 10 °C/min under oxygen gas until an exothermic change was observed. The OIT_{temp} was reported at an onset temperature of the exothermic change.

Antibacterial activity of neat PBS and its composite films was conducted in accordance with ISO 22196:2011. The test was carried out against gram positive and gram negative bacteria of Staphylococcus aureus (*S.* aureus, ATCC 6538p) and Escherichia coli (*E.* coli, ATCC 8739), respectively. The antibacterial activity (R) of the films was calculated as follows:

$$R = U_t - A_t \qquad (4)$$

where U_t and A_t are the average of the logarithm of the number of viable bacteria (CFU/cm^2) from neat PBS and each PBS/lignin composite film, respectively. The reduction in percentage was calculated using Eq. (5):

$$Reduction(\%) = \left(\frac{B-C}{B} \times 100\right) \qquad (5)$$

where B and C are the average of the number of viable bacteria (cells/cm^2) recovered from the neat PBS and each PBS/lignin composite film after 24 hours.

3. Results And Discussion

The visual appearance of the S-lignin was an agglomerated dark-brown powder. The morphology observed by SEM is shown in Fig. 2 (a). The agglomerated particles were irregular in shape and sizes varied from a few microns to 50 µm. Ash content of softwood kraft lignin was 1.22%, which was in the same range as those reported previously [45–47]. In this work, purification and molecular weight

fractionation using acetone was performed to reduce ash content in the S-lignin. Yield of acetone-soluble fraction was approximately 59%.

S-LNPs were prepared in two steps: purification of lignin using organic solvent (acetone) and production of S-LNPs via anti-solvent precipitation assisted with ultrasonication. The obtained S-LNPs has a lower ash content of 0.05% as compared to 1.22% of the S-lignin. This can be due to the fact that inorganics in S-lignin such as sulphur, sodium, silicon are not able to dissolve in acetone [48, 49]. Figure 2 (b) shows SEM micrograph of spherical lignin particles of the S-LNPs. A representative particle size distribution is displayed in Fig. 2 (c). The size of S-LNPs was found in the range of 40–300 nm and the average particle size from 5 runs was 120 ± 18 nm and the average PDI was 0.07 ± 0.01. A simple mechanism of the S-LNPs formation in this work can be explained by the amphiphilic character of lignin, composed of hydrophilic groups (such as hydroxyls a carboxyls) and hydrophobic groups (such as phenolic rings). Dissolving lignin in an organic solvent such as acetone, methanol, ethanol results in breaking the weak hydrogen bond between its molecules. Hydrophobic side of lignin molecules turns to aggregate when surrounded with antisolvent such as deionized water. The small aggregate acts as a nucleus and builds gradually by the formation of layer-by-layer of lignin molecules via the aromatic π-π interactions. Hydrophilic side (hydroxyl and carboxyl groups) forms naturally on the surface of the aggregate and lignin nanoparticles in spherical shape are attained in order to minimize the overall interface area with antisolvent (deionized water) molecules [36, 50, 51]. In the work, ultrasonication energy was applied during the formation of lignin nanoparticles to attain small particles of S-LNPs. Partially formed lignin nanoparticles were collapsed by static pressure generated from sonication probe, as illustrated in Fig. 1. Once the resultant lignin particles were completely formed, the particles were stable and suspended in deionized water.

Glass transition temperature (T_g) of S-LNPs was detected at 146 °C, which is 17 °C lower than that of S-lignin (Table 1). The reducing in ash content and T_g of S-LNPs was related to its origin where acetone-soluble lignin used for the preparation of S-LNPs. Soluble-fraction obtained from fractionation using organic solvents such as methanol, ethanol, propanol and acetone has been reported to have lower ash content, molecular weight and T_g as compared to its parent lignin [52–55].

Chemical structures of S-lignin and S-LNPs were determined by ^{31}P NMR spectroscopy. In Fig. 3 (a), three key constituents of aliphatic, phenolic and carboxylic hydroxyls were detected in both S-lignin and S-LNPs samples. In the region of phenolic hydroxyl, 137.6 to 144.0 ppm, only guaiacyl and *p*-hydroxyphenyl hydroxyls were observed without any signal of syringyl hydroxyl in C_5-substitutent hydroxyl region (see Fig. 3 (b)). Inter-monolignolic linkages of lignin such as pheylcoumaran (β-5’), biphenyl (5–5’) and ether linkage of β-Aryl ether (β-O-4’) were identified in both S-lignin and S-LNPs samples. Internal standard, NHND, was used for quantitative analysis of each constituent. The quantitative results are compiled in Table 1. Type and content of phenolic hydroxy contained in lignin are varied and depended on its plant taxonomy. S-lignin possessed the greatest guaiacyl hydroxyl group at 1.26 mmol/g contributing about 96% of total monolignol which was the character of softwood lignin [12, 45]. Guaiacyl hydroxyl group

was increased to 1.37 mmol/g in S-LNPs. A ratio of phenolic to aliphatic hydroxyl groups of S-lignin was 1.1 and it was increased to 1.7 for S-LNPs. High content of phenolic hydroxy group has been reported to exhibit better in active functions of lignin including UV-blocking, antioxidant and anti-microbial abilities [56–58].

Table 1
Functional groups and glass transition temperature (T_g) of S-lignin and S-LNPs.

Samples	Aliphatic-OH	Phenolic-OH (mmol/g)			COOH	T_g
	(mmol/g)	C_5-substituted	Guaiacyl	p-hydroxyphenyl	(mmol/g)	(°C)
S-lignin	1.69	0.50	1.26	0.05	0.38	163
S-LNPs	1.19	0.61	1.37	0.01	0.42	146

Using acetone to purify S-lignin and producing S-LNPs demonstrated in this work can reduce inorganic containing in S-lignin and enhance a portion of phenolic hydroxyl. It can be suggested that the production of S-LNPs using acetone is a simple and green process as compared to relatively toxic solvents such as tetrahydrofuran (THF), ethylene glycol, and dioxane, used in literature. The majority of the publications producing lignin nanoparticles uses THF [59–62], ethylene glycol [63–66] and dioxane [67, 68]. Some publications reported on using an acid precipitation to produce lignin nanoparticles [69, 70]. Manipulation of the above solvents, aqueous solutions, or acidified water is more complicated and expensive than using acetone. Moreover, acetone from fractionation and production of S-LNPs can be recovered by solvent evaporator and the recovered acetone can be reused.

Neat PBS films, and its composite films of PBS/S-lignin and PBS/S-LNPs were prepared by the conventional blown film extrusion.

Figure 4 (a) shows white milky neat PBS film and brownish composite films incorporated with S-LNPs. An increasing S-LNPs significantly affected color of the composite films. The same brownish trend was observed on the PBS/S-lignin composite films. Film color was identified by Commission Internationale de l'Eclairage (CIE) system. L*, a*, b* coordinates of neat PBS were 91.35, -0.56, 10.66. This indicated white with high lightness. Color change, ΔL*, Δa*, Δb*, of the PBS/lignin composite films was determined based on the coordinates of the neat PBS film (see Fig. 5 (a) and (b)). Obvious increase in Δb* and decrease in ΔL* with increase lignin contents were found in both PBS/S-lignin and PBS/S-LNPs composite films. This indicated that the composite films became darker and yellower, corelating well with the appearance of the composite films presented in

Figure 4 (a).

Figure 4 (b) shows a photograph of monolayer films placed over texts. The neat PBS films was transparent and homogeneous. After incorporation of either S-lignin or S-LNPs, the composite films were

still transparent and the visual appearance was well matched with the L value ranging from 91 to 82. These findings were consistent with literature [19, 23, 24, 44, 71]. Color difference (ΔE) values of the PBS/S-lignin composite films with 0.1, 0.2, 0.5 and 1.0 wt% were 1.5, 2.7, 5.5 and 8.7, respectively and slightly higher ΔE of 1.9, 3.4, 6.7 and 9.6 for the PBS/S-LNPs composite films.

Figure 4 (c) shows optical micrographs of the neat PBS and the composite films. Brown particles were observed in PBS/S-lignin composite films whereas the neat PBS and PBS/S-LNPs showed no contrast indicating homogeneous S-LNPs distributed in the PBS films. The nano scale of S-LNPs might result in higher ΔE as compared to the composite films of PBS/S-lignin. Good dispersion and distribution of lignin particles could impact properties of the resultant composite films especial for mechanical and functional properties.

Thermal properties of the resultant films were examined, DSC thermograms obtained from the 1st cooling scan and the 2nd heating scan of the neat PBS, PBS/S-lignin_0.5 and PBS/S-LNPs_0.5 films are overlaid and shown in Figure 6 (a) and Figure 6 (b), respectively. The determined melting temperature (T_m), crystallization temperature (T_c) and crystallinity (X_c) are compiled in Table 2. The neat PBS film exhibited T_c at approximately 89 °C. Two melting peaks at 110 °C and 117 °C were detected during heating process which correlated well with the result reported in literature [72–74]. No significant change in crystallization and T_c was detected in both PBS/lignin composite films, whereas melting of the crystallized PBS was changed remarkably when compared to the neat PBS film. The first melting temperatures of crystalline PBS (T_{m1}) obtained from both PBS/lignin composite films (PBS/S-linin and PBS-LNPs) were observed clearly at 108 °C and it was lower than that of the neat PBS (at 110 °C). This indicated that the formation of smaller crystalline PBS was induced by adding of lignin particles. Moreover, the second melting peak (T_{m2}) obtained from the PBS/lignin composite films at approximate 114 °C was sharper and lower than that of the neat PBS film. This is consistent with the smaller crystalline PBS examined from T_{m1}. These results suggest that a growth of PBS spherulite might be disrupted by added lignin particles. As shown in Figure 6 (b), an integral area under endothermic peaks represents crystallinity (X_c) in the resultant films. The X_c of neat PBS film was 26 %. X_c of PBS tended to slightly increase to 27% when PBS was incorporated with lignin. Slightly increase of X_c reported in this work could be explained due to the small amount below 1.0 wt% of lignin was loaded into the PSB matrix. Figure 6 (c) and Figure 6 (d) show DSC thermograms of PBS films with different S-LNPs contents at 0.1, 0.5 and 1.0 wt%. There was no significant change in the profile of heat flow and all the examined T_c, T_m and X_c. Obvious increase in X_c of biodegradable polyester-based polymer including PLA [75], PHB [76] and PBAT [77] has been demonstrated when using high amount of lignin. Overall, results from the DSC analysis show that loading of lignin (both S-lignin and S-LNPs) ranges from 0.1 to 1.0 wt% has no negative effect on the thermal properties of PBS films. Mechanical properties and other active functions including UV-shielding, antioxidation and antibacterial abilities are demonstrated in the following sections.

Table 2
Thermal properties of the neat PBS film and its composite films.

Samples	First cooling scan		Second heating scan		
	Onset T_c (°C)	T_c (°C)	T_{m1} (°C)	T_{m2} (°C)	X_c(%)
Neat PBS	93.0	88.8	110.0	117.1	25.8
PBS/S-lignin_0.5	92.9	89.2	108.1	114.5	26.4
PBS/S-LNP_S_0.5	93.2	89.1	107.8	114.8	27.1
PBS/S-LNP_S_0.1	92.9	89.3	107.5	114.2	26.5
PBS/S-LNP_S_1.0	93.4	89.4	107.9	115.7	26.8

The conventional blown film extrusion was employed to fabricate neat PBS film and its composite films. Mechanical properties including Young's modulus, tensile strength and elongation at break of the resultant films were evaluated for machine direction (MD) and transverse direction (TD) and the results are summarized in Table 3. Mechanical properties in both MD and TD are regularly informed for flexible film application. Neat PBS exhibited Young's modulus, tensile strength and elongation at break in MD at 321 MPa, 35 MPa and 296 %, respectively. Those in TD were 390 MPa, 34 MPa and 96%, respectively. Tukey tests were conducted at a significant difference at p value < 0.05 (95% confidence interval). PBS composite films with S-LNPs at 0.1 and 0.5 wt% exhibited significant improvement in Young's modulus in MD as compared to the neat PBS and PBS/S-lignin_0.5 films. Increased Young's modulus observed in this study is in good agreement to other polymers reported in literature [8, 75–77]. Young's modulus was drop and the value was comparable to the neat PBS and PBS/S-lignin_0.5 films, when the content of S-LNPs increased to 1.0 wt%. This might be due to the high loading content of S-LNPs. Considering the PBS composite films at same loading content of 0.5 wt% (PBS/S-lignin_0.5 and PBS/S-LNPs_0.5), the PBS/S-LNPs_0.5 had significant higher Young's modulus in MD of 358 MPa, tensile strength in MD of 33.2 MPa, and elongation at break in TD of 93% than those obtained from PBS/S-lignin_0.5. This is highly possible due to small size and uniform shape of S-LNPs that influencing the dispersion and distribution in PBS matrix. Moreover, this correlates well with good dispersion without agglomeration of SLPs observed under optical microscope displayed previously in

Figure 4 (c). Moreover, mechanical properties in both MD and TD of PBS/S-LNPs composite film at 0.5 wt% were similar to the neat PBS. These results suggest that using S-LNPs at 0.5 wt% does not deteriorate the tensile properties of PBS film.

Table 3
Tensile properties of neat PBS film and the PBS/lignin composite films.

Samples	Testing directions	Young's modulus (MPa)		Tensile strength (MPa)		Elongation at break (%)	
		Ave.	S.D.	Ave.	S.D.	Ave.	S.D.
Neat PBS	MD	321.5^{b}	23.1	$34.5^{a,b}$	1.8	296.1^{a}	14.8
	TD	390.4^{a}	20.5	33.9^{a}	1.1	95.7^{a}	24.4
PBS/S-lignin_0.5	MD	312.4^{b}	22.9	30.1^{c}	2.1	243.5^{b}	34.1
	TD	390.7^{a}	33.3	27.7^{b}	2.6	35.7^{b}	5.9
PBS/S-LNPs_0.5	MD	358.1^{a}	12.3	33.2^{a}	2.0	$293.1^{a,b}$	9.5
	TD	368.6^{a}	19.6	$29.6^{a,b}$	2.0	93.4^{a}	25.7
PBS/S-LNPs_0.1	MD	329.0^{a}	23.2	$32.2^{b,c}$	1.7	$291.5^{a,b}$	37.6
	TD	359.7^{a}	15.2	27.7^{b}	3.0	90.7^{a}	19.4
PBS/S-LNPs_1.0	MD	318.8^{b}	18.8	30.9^{c}	2.2	$283.5^{a,b}$	10.5
	TD	384.4^{a}	10.2	$29.8^{a,b}$	3.0	59.8^{b}	20.1

UV-visible transmittance of the neat PBS and its composite films containing different contents of lignins is shown in Fig. 7 (a and b). The neat PBS film exhibited nearly transparent at 88 ± 0.52% transmittance in visible region (wavelength range of 400 to 800 nm). However, the neat PBS film showed a poor UV-shielding property as it could not absorb UV radiation (wavelength of 280–400 nm), having high UV transmittance of 95 ± 0.91%. Addition of either S-lignin or S-LNPs at the content of 0.5 wt% had no significant effect on transmittance in visible region where the transmittance was 87–88%. At the lignin content of 1.0 wt%, the PBS/S-lignin and the PBS/S-LNPs composite films became 84 and 85% transmittance, respectively. The transmittance of the composite films reduced significantly in both UVA (315–400 nm) and UVB (280–315 nm) regions. In case of PBS/S-lignin composite films shown in Fig. 7 (a), UV transmittance of the films containing 0.1, 0.2, 0.5 and 1.0 wt% were reduced to 91%, 84%, 67% and 47%, respectively. The higher reducing trend was seen for PBS/S-LNPs composite films, 85%, 75%, 54% and 40% at the films containing 0.1, 0.2, 0.5 and 1.0 wt%, respectively (see Fig. 7 (b)). Figure 7 (c) shows an overlaid light transmission of all three groups: neat PBS (bold black line), PBS/S-lignin composite films (blue lines) and PBS/S-LNPs (red lines). At the same loading contents, PBS/S-LNPs composite films possessed better UV-shielding ability as compared to PBS/S-lignin composite films. This attributed to S-LNPs high surface area and better dispersion. Enhancement (%) was calculated using PBS/S-lignin composite films as references, the enhancements of the composite films with S-LNPs at 0.1, 0.5 and 1.0

wt% were 10%, 19% and 14% respectively. This could be said that 0.5 wt% was the optimum loading content of S-LNPs based on the UV-shielding results.

Figure 8 (a) shows the DSC thermograms to evaluate an oxidation induction temperature (OIT_{temp}). An endothermic peak at approximate 115 °C was detected in all films. This revealed the melting character of PBS. During heating under the presence of oxygen, all of the films exhibited an exothermic behaviour. The onset OIT_{temp} of neat PBS film was 198 °C, while that of PBS/lignin composite films with 0.5 wt% of lignin was retarded to the temperature close to 300 °C as shown in Fig. 8 (b). PBS film with S-LNPs displayed significant high onset OIT_{temp} at 284°C while the PBS film with S-lignin had the onset OIT_{temp} at 279°C. The oxidative stabilization action of the S-lignin and S-LNPs manifested as the onset OIT_{temp} was correlated well with the portion of phenolic hydroxyl of the lignin [56]. S-LNPs with 1.99 mmol/g of phenolic hydroxyl performed better oxidative stabilization than S-lignin containing 1.85 mmol/g of phenolic hydroxyl See the aforementioned results compiled in Table 1. Moreover, good dispersion and distribution of S-LNPs in the PBS matrix might be another factor enhancing the onset OIT_{temp}.

Antimicrobial ability is one of the active functions of lignin, relating to the structure of polyphenol in lignin. From literature, lignin has been reported extensively to manufacture antimicrobial materials for sustainable, hygiene, and active packaging. However, commercial bioplastic has no antimicrobial ability. Therefore, incorporation of lignin into bioplastic had been explored in order to preserve fully bioplastic composites and enhance antimicrobial ability. For example lab-prototype films such as agar [26], starch-based polymer [78] and cellulose[79] and commercial bioplastic such as PLA[75], PBAT [77], PHB[76] and PBS[22] have been investigated for antimicrobial ability when incorporated with lignin. In this research, antibacterial ability of the surface of PBS/lignin composite films was performed with two types of bacteria, *E.* coli and *S.* aureus representing gram negative and positive bacterial, respectively. Results obtained from the measurement in accordance with ISO 22196:2011 are compiled in Table 4 Considering the antibacterial ability of *E.*coli, the neat PBS film exhibited the highest average of the number of viable bacteria per 1 cm^2 at 3.94×10^4, while the PBS/S-lignin and PBS/S-LNPs films at 0.5 wt% of loading content displayed decreased number of viable bacteria to 1.36×10^3 and 1.26×10^2, respectively. This indicates the antibacterial ability of PBS film is enhanced by adding small amount of lignin. At the same concentration of loaded lignin (0.5 wt%), PBS/S-LNPs films demonstrated more effective antibacterial ability against gram-negative bacteria (*E.* coli) at the highest R value of 2.5 and % reduction of 99.7 when compared to PBS/S-lignin. This relates to its higher phenolic hydroxyl group that is capable of destroying the bacterial cell walls through the reactive oxygen species (ROS) mechanism, which was proposed in literature [80–82].

Table 4
Antibacterial ability against E. coli (ATCC 8739) and S. aureus (ATCC 6538p) of the neat PBS, PBS/S-lignin and PBS/S-LNPs films.

Samples	The average of the number of viable bacteria/ cm^2	The average of the common logarithm of the number of viable bacteria/ cm^2	Antibacterial activity (R)	%Reduction
E. coli (ATCC 8739)				
Neat PBS	$3.94 \cdot 10^4$	4.60	NA	NA
PBS/S-lignin_0.5	$1.36 \cdot 10^3$	3.13	1.5	96.6
PBS/S-LNPs_0.5	$1.26 \cdot 10^2$	2.10	2.5	99.7
S. aureus (ATCC 6538p)				
Neat PBS	$8.88 \cdot 10^3$	3.95	NA	NA
PBS/S-lignin_0.5	$3.12 \cdot 10^2$	2.49	1.5	96.5
PBS/S-LNPs_0.5	$3.09 \cdot 10^2$	2.49	1.5	96.5

In summary, we demonstrated a simple and green procedure to produce lignin nanoparticles, S-LNPs, that used friendly conventional blown film extrusion. Attained lignin nanoparticles acted as multifunctional additives for bioplastic PBS flexible film. This related to the presence of the phenolic OH groups within lignin that promoted efficiently in UV-shielding ability, thermo-antioxidative reaction and antibacterial ability. The processability and mechanical properties of the lignin nanocomposite films were similar to the neat PBS film.

4. Conclusions

In this work, spherical lignin nanoparticles were manufactured by a simple and green protocol. Organic solvent, acetone, was selected for fractionation in order to remove inorganic impurity and purify the pristine lignin (S-lignin) and phenolic hydroxyl content within the purified lignin was increased. The purified lignin was converted to spherical lignin nanoparticles (S-LNPs) via antisolvent precipitation assisted by ultrasonication. The attained S-LNPs were incorporated into biodegradable polyester-based polymer, polybutylene succinate (PBS) without any modification via the conventional blown film extrusion. Adding of S-LNPs did not restrict the film processability. The composite film with 0.5 wt% of S-LNPs (PBS/S-LNPs_0.5) exhibited comparable thermal and mechanical properties to the neat PBS film. Significant improvement on UV-shielding ability, antioxidation and antibacterial were achieved with small amount of SLPs (0.5 wt%), while the film transparency was still satisfied. From the overall results, we demonstrated a practical and friendly process to produce spherical lignin nanoparticles that were composited with PBS by the conventional blown film extrusion. The fully biodegradable composite

PBS/S-LNPs films with active functions of superior UV protection, antioxidation and antibacterial abilities can be alternative choices for food products that sensitive from UV light.

Declarations

Acknowledgments

Authors appreciate the support from National Metal and Materials Technology Center (MTEC), National Science and Technology Development Agency (NSTDA), Thailand. Authors wish to acknowledge Prof. Dr. S. Seraphin, Professional Authorship Center (PAC), NSTDA for useful suggestions.

Funding

Authors appreciate the funding support from National Metal and Materials Technology Center (MTEC), National Science and Technology Development Agency (NSTDA), Thailand (No.2052415).

Declaration of competing interest

The authors declare that they have no known competing financial interests or personal relationships that could have appeared to influence the work reported in this paper.

CRediT authorship contribution statement

Bongkot Hararak: Conceptualization, Methodology, Investigation, Formal analysis, Project administration, Validation, Writing - review & editing, Supervision, Funding acquisition. **Charinee Winotapun:** Conceptualization, Methodology, Investigation, Formal analysis, Funding acquisition. **Natcha Prakymoramas:** Conceptualization, Methodology, Investigation, Formal analysis, Funding acquisition. **Pawarisa Wijaranakul:** Methodology, Investigation, Formal analysis.

References

1. Coversio Market and strategy (2020) Plastic flow 2018. https://www.bkv-gmbh.de/files/bkv-neu/studien/Global_Plastics_Flow_Feb10_2020.pdf
2. Plastic europe (2020) Plastics – the Facts 2020
3. Chatterjee S, Sharma S (2019) Microplastics in our oceans and marine health.F Actions Sci Reports54–61
4. Sridharan S, Kumar M, Singh L et al (2021) Microplastics as an emerging source of particulate air pollution: A critical review. J Hazard Mater 418:126245. https://doi.org/https://doi.org/10.1016/j.jhazmat.2021.126245
5. Jamieson AJ, Brooks LSR, Reid WDK et al (2019) Microplastics and synthetic particles ingested by deep-sea amphipods in six of the deepest marine ecosystems on Earth. R Soc Open Sci 6:180667. https://doi.org/10.1098/rsos.180667

6. Zhou S-J, Wang H-M, Xiong S-J et al (2021) Technical Lignin Valorization in Biodegradable Polyester-Based Plastics (BPPs). ACS Sustain Chem Eng 9:12017–12042. https://doi.org/10.1021/acssuschemeng.1c03705
7. Bioplastics European (2022) Bioplastics facts and figures. https://docs.european-bioplastics.org/publications/EUBP_Facts_and_figures.pdf
8. Zhang Y, Zhou S, Fang X et al (2019) Renewable and flexible UV-blocking film from poly(butylene succinate) and lignin. Eur Polym J 116:265–274. https://doi.org/https://doi.org/10.1016/j.eurpolymj.2019.04.003
9. Kim H-S, Yang H-S, Kim H-J (2005) Biodegradability and mechanical properties of agro-flour–filled polybutylene succinate biocomposites. J Appl Polym Sci 97:1513–1521. https://doi.org/https://doi.org/10.1002/app.21905
10. Platnieks O, Gaidukovs S, Barkane A et al (2020) Bio-Based Poly(butylene succinate)/Microcrystalline Cellulose/Nanofibrillated Cellulose-Based Sustainable Polymer Composites: Thermo-Mechanical and Biodegradation Studies. Polymers (Basel) 12:. https://doi.org/10.3390/polym12071472
11. Lin N, Fan D, Chang PR et al (2011) Structure and properties of poly(butylene succinate) filled with lignin: A case of lignosulfonate. J Appl Polym Sci 121:1717–1724. https://doi.org/https://doi.org/10.1002/app.33754
12. Calvo-Flores FG, Dobado JA, Isac-García J, Martín-Martínez FJ (2015) Lignin and Lignans as Renewable Raw Materials: Chemistry, Technology and Applications. John Wiley & Sons Ltd
13. Miller J, Faleiros M, Bodart L, Bodart A-C (2016) Lignin:Technology, Applications and Markets
14. Vasile C, Cazacu G (2013) Biocomposites and Nanocomposites Containing Lignin. In: Dufresne A, Sabu T, Pothen LA (eds) Biopolymer Nanocomposites. John Wiley & Sons, Inc., pp 565–598
15. Bajpai P (2016) Pretreatment of Lignocellulosic Biomass for Biofuel Production. Springer Singapore, Singapore
16. Melro E, Alves L, Antunes FE, Medronho B (2018) A brief overview on lignin dissolution. J Mol Liq 265:578–584. https://doi.org/https://doi.org/10.1016/j.molliq.2018.06.021
17. Köhnke J, Rennhofer H, Lichtenegger H et al (2018) Electrically Conducting Carbon Microparticles by Direct Carbonization of Spent Wood Pulping Liquor. ACS Sustain Chem Eng 6:3385–3391. https://doi.org/10.1021/acssuschemeng.7b03582
18. Barana D, Ali SD, Salanti A et al (2016) Influence of Lignin Features on Thermal Stability and Mechanical Properties of Natural Rubber Compounds. ACS Sustain Chem Eng 4:5258–5267. https://doi.org/10.1021/acssuschemeng.6b00774
19. Zhang X, Liu W, Liu W, Qiu X (2020) High performance PVA/lignin nanocomposite films with excellent water vapor barrier and UV-shielding properties. Int J Biol Macromol 142:551–558. https://doi.org/https://doi.org/10.1016/j.ijbiomac.2019.09.129
20. Yang W, Owczarek JS, Fortunati E et al (2016) Antioxidant and antibacterial lignin nanoparticles in polyvinyl alcohol/chitosan films for active packaging. Ind Crops Prod 94:800–811.

https://doi.org/https://doi.org/10.1016/j.indcrop.2016.09.061

21. Yang W, Fortunati E, Dominici F et al (2016) Effect of cellulose and lignin on disintegration, antimicrobial and antioxidant properties of PLA active films. Int J Biol Macromol 89:360–368. https://doi.org/https://doi.org/10.1016/j.ijbiomac.2016.04.068
22. Domínguez-Robles J, Larrañeta E, Fong ML et al (2020) Lignin/poly(butylene succinate) composites with antioxidant and antibacterial properties for potential biomedical applications. Int J Biol Macromol 145:92–99. https://doi.org/https://doi.org/10.1016/j.ijbiomac.2019.12.146
23. Tian D, Hu J, Bao J et al (2017) Lignin valorization: lignin nanoparticles as high-value bio-additive for multifunctional nanocomposites. Biotechnol Biofuels 10:192. https://doi.org/10.1186/s13068-017-0876-z
24. Kim Y, Suhr J, Seo H-W et al (2017) All Biomass and UV Protective Composite Composed of Compatibilized Lignin and Poly (Lactic-acid). Sci Rep 7:43596. https://doi.org/10.1038/srep43596
25. Ye D, Li S, Lu X et al (2016) Antioxidant and Thermal Stabilization of Polypropylene by Addition of Butylated Lignin at Low Loadings. ACS Sustain Chem Eng 4:5248–5257. https://doi.org/10.1021/acssuschemeng.6b01241
26. Zadeh EM, O'Keefe SF, Kim Y-T (2018) Utilization of Lignin in Biopolymeric Packaging Films. ACS Omega 3:7388–7398. https://doi.org/10.1021/acsomega.7b01341
27. Schorr D, Diouf PN, Stevanovic T (2014) Evaluation of industrial lignins for biocomposites production. Ind Crops Prod 52:65–73. https://doi.org/10.1016/j.indcrop.2013.10.014
28. Gao W, Fatehi P (2019) Lignin for polymer and nanoparticle production: Current status and challenges. Can J Chem Eng 97:2827–2842. https://doi.org/10.1002/cjce.23620
29. Luo S, Cao J, McDonald AG (2016) Interfacial Improvements in a Green Biopolymer Alloy of Poly(3-hydroxybutyrate-co-3-hydroxyvalerate) and Lignin via in Situ Reactive Extrusion. ACS Sustain Chem Eng 4:3465–3476. https://doi.org/10.1021/acssuschemeng.6b00495
30. Chile L-E, Kaser SJ, Hatzikiriakos SG, Mehrkhodavandi P (2018) Synthesis and Thermorheological Analysis of Biobased Lignin-graft-poly(lactide) Copolymers and Their Blends. ACS Sustain Chem Eng 6:1650–1661. https://doi.org/10.1021/acssuschemeng.7b02866
31. Tajeddin B, Arabkhedri M (2020) Polymers and food packaging. In: AlMaadeed MAA, Ponnamma D, Carignano MA (eds) Polymer Science and Innovative Applications. Elsevier, pp 525–543
32. Breil J (2011) Future trends for biaxially oriented films and orienting lines. In: DeMeuse MT (ed) Biaxial Stretching of Film. Woodhead Publishing, pp 240–273
33. Roopan SM (2017) An overview of natural renewable bio-polymer lignin towards nano and biotechnological applications. Int J Biol Macromol 103:508–514. https://doi.org/https://doi.org/10.1016/j.ijbiomac.2017.05.103
34. Chauhan PS (2020) Lignin nanoparticles: Eco-friendly and versatile tool for new era. Bioresour Technol Reports 9:100374. https://doi.org/https://doi.org/10.1016/j.biteb.2019.100374

35. Beisl S, Friedl A, Miltner A (2017) Lignin from Micro- to Nanosize: Applications. Int J Mol Sci 18. https://doi.org/10.3390/ijms18112367
36. Österberg M, Sipponen MH, Mattos BD, Rojas OJ (2020) Spherical lignin particles: a review on their sustainability and applications. Green Chem 22:2712–2733. https://doi.org/10.1039/D0GC00096E
37. Shankar S, Reddy JP, Rhim J-W (2015) Effect of lignin on water vapor barrier, mechanical, and structural properties of agar/lignin composite films. Int J Biol Macromol 81:267–273. https://doi.org/https://doi.org/10.1016/j.ijbiomac.2015.08.015
38. Liu R, Dai L, Hu L-Q et al (2017) Fabrication of high-performance poly(l-lactic acid)/lignin-graft-poly(d-lactic acid) stereocomplex films. Mater Sci Eng C Mater Biol Appl 80:397–403. https://doi.org/10.1016/j.msec.2017.06.006
39. Hararak B, Winotapun C, Inyai J et al (2021) Production of UV-shielded spherical lignin particles as multifunctional bio-additives for polyvinyl alcohol composite films. J Nanoparticle Res 23:193. https://doi.org/10.1007/s11051-021-05308-z
40. Xing Q, Buono P, Ruch D et al (2019) Biodegradable UV-Blocking Films through Core–Shell Lignin–Melanin Nanoparticles in Poly(butylene adipate-co-terephthalate). ACS Sustain Chem Eng 7:4147–4157. https://doi.org/10.1021/acssuschemeng.8b05755
41. Meng X, Crestini C, Ben H et al (2019) Determination of hydroxyl groups in biorefinery resources via quantitative 31 P NMR spectroscopy. Nat Protoc 14:2627–2647. https://doi.org/10.1038/s41596-019-0191-1
42. Li N, Chen Y, Yu H et al (2017) Evaluation of optical properties and chemical structure changes in enzymatic hydrolysis lignin during heat treatment. RSC Adv 7:20760–20765. https://doi.org/10.1039/C7RA02005H
43. Zhu W, Wang X, Chen X, Xu K (2009) Miscibility, crystallization, and mechanical properties of poly(3-hydroxybutyrate-co-4-hydroxybutyrate)/ poly(butylene succinate) blends. J Appl Polym Sci 114:3923–3931. https://doi.org/https://doi.org/10.1002/app.30965
44. He X, Luzi F, Hao X et al (2019) Thermal, antioxidant and swelling behaviour of transparent polyvinyl (alcohol) films in presence of hydrophobic citric acid-modified lignin nanoparticles. Int J Biol Macromol 127:665–676. https://doi.org/https://doi.org/10.1016/j.ijbiomac.2019.01.202
45. Hu Z, Du X, Liu J et al (2016) Structural Characterization of Pine Kraft Lignin: BioChoice Lignin vs Indulin AT. J Wood Chem Technol 36:432–446. https://doi.org/10.1080/02773813.2016.1214732
46. Dodd AP, Kadla JF, Straus SK (2015) Characterization of fractions obtained from two industrial softwood kraft lignins. ACS Sustain Chem Eng 3:103–110. https://doi.org/10.1021/sc500601b
47. Jiang X, Savithri D, Du X et al (2017) Fractionation and Characterization of Kraft Lignin by Sequential Precipitation with Various Organic Solvents. ACS Sustain Chem Eng 5:835–842. https://doi.org/10.1021/acssuschemeng.6b02174
48. Mandlekar N, Cayla A, Rault F et al (2018) An Overview on the Use of Lignin and Its Derivatives in Fire Retardant Polymer Systems. In: Poletto M (ed) Lignin - Trends and Applications. IntechOpen, Rijeka

49. Chung H, Washburn NR (2015) Extraction and Types of Lignin. In: Lignin in Polymer Composites. pp 13–25
50. Schneider WDH, Dillon AJP, Camassola M (2021) Lignin nanoparticles enter the scene: A promising versatile green tool for multiple applications. Biotechnol Adv 47:107685. https://doi.org/https://doi.org/10.1016/j.biotechadv.2020.107685
51. Tian D, Hu J, Chandra RP et al (2017) Valorizing Recalcitrant Cellulolytic Enzyme Lignin via Lignin Nanoparticles Fabrication in an Integrated Biorefinery. ACS Sustain Chem Eng 5:2702–2710. https://doi.org/10.1021/acssuschemeng.6b03043
52. Tagami A, Gioia C, Lauberts M et al (2019) Solvent fractionation of softwood and hardwood kraft lignins for more efficient uses: Compositional, structural, thermal, antioxidant and adsorption properties. Ind Crops Prod 129:123–134. https://doi.org/10.1016/j.indcrop.2018.11.067
53. Jääskeläinen AS, Liitiä T, Mikkelson A, Tamminen T (2017) Aqueous organic solvent fractionation as means to improve lignin homogeneity and purity. Ind Crops Prod 103:51–58. https://doi.org/10.1016/j.indcrop.2017.03.039
54. Domínguez-Robles J, Tamminen T, Liitiä T et al (2018) Aqueous acetone fractionation of kraft, organosolv and soda lignins. Int J Biol Macromol 106:979–987. https://doi.org/10.1016/j.ijbiomac.2017.08.102
55. Park SY, Kim J-Y, Youn HJ, Choi JW (2018) Fractionation of lignin macromolecules by sequential organic solvents systems and their characterization for further valuable applications. Int J Biol Macromol 106:793–802. https://doi.org/10.1016/j.ijbiomac.2017.08.069
56. Sadeghifar H, Argyropoulos DS (2015) Correlations of the Antioxidant Properties of Softwood Kraft Lignin Fractions with the Thermal Stability of Its Blends with Polyethylene. ACS Sustain Chem Eng 3:349–356. https://doi.org/10.1021/sc500756n
57. Guo Y, Tian D, Shen F et al (2019) Transparent Cellulose/Technical Lignin Composite Films for Advanced Packaging. Polym (Basel) 11:1455. https://doi.org/10.3390/polym11091455
58. Lourençon TV, de Lima GG, Ribeiro CSP et al (2021) Antioxidant, antibacterial and antitumoural activities of kraft lignin from hardwood fractionated by acid precipitation. Int J Biol Macromol 166:1535–1542. https://doi.org/https://doi.org/10.1016/j.ijbiomac.2020.11.033
59. Salentinig S, Schubert M (2017) Softwood Lignin Self-Assembly for Nanomaterial Design. Biomacromolecules 18:2649–2653. https://doi.org/10.1021/acs.biomac.7b00822
60. Mattinen M-L, Riviere G, Henn A et al (2018) Colloidal Lignin Particles as Adhesives for Soft Materials. Nanomaterials 8:. https://doi.org/10.3390/nano8121001
61. Lievonen M, Valle-Delgado JJ, Mattinen M-L et al (2016) A simple process for lignin nanoparticle preparation. Green Chem 18:1416–1422. https://doi.org/10.1039/C5GC01436K
62. Sipponen MH, Smyth M, Leskinen T et al (2017) All-lignin approach to prepare cationic colloidal lignin particles: stabilization of durable Pickering emulsions. Green Chem 19:5831–5840. https://doi.org/10.1039/C7GC02900D

63. Richter AP, Bharti B, Armstrong HB et al (2016) Synthesis and Characterization of Biodegradable Lignin Nanoparticles with Tunable Surface Properties. Langmuir 32:6468–6477. https://doi.org/10.1021/acs.langmuir.6b01088
64. Yang W, Rallini M, Wang D-Y et al (2018) Role of lignin nanoparticles in UV resistance, thermal and mechanical performance of PMMA nanocomposites prepared by a combined free-radical graft polymerization/masterbatch procedure. Compos Part A Appl Sci Manuf 107:61–69. https://doi.org/https://doi.org/10.1016/j.compositesa.2017.12.030
65. Yang W, Fortunati E, Bertoglio F et al (2018) Polyvinyl alcohol/chitosan hydrogels with enhanced antioxidant and antibacterial properties induced by lignin nanoparticles. Carbohydr Polym 181:275–284. https://doi.org/https://doi.org/10.1016/j.carbpol.2017.10.084
66. Frangville C, Rutkevičius M, Richter AP et al (2012) Fabrication of Environmentally Biodegradable Lignin Nanoparticles. ChemPhysChem 13:4235–4243. https://doi.org/10.1002/cphc.201200537
67. Qian Y, Deng Y, Qiu X et al (2014) Formation of uniform colloidal spheres from lignin, a renewable resource recovered from pulping spent liquor. Green Chem 16:2156–2163. https://doi.org/10.1039/C3GC42131G
68. Li H, Deng Y, Wu H et al (2016) Self-assembly of kraft lignin into nanospheres in dioxane-water mixtures. Holzforschung 70:725–731. https://doi.org/doi:10.1515/hf-2015-0238
69. Azimvand J, Didehban K, Mirshokrai S (2018) Preparation and Characterization of Lignin Polymeric Nanoparticles Using the Green Solvent Ethylene Glycol: Acid Precipitation Technology. BioResources 13:2887–2897. https://doi.org/10.15376/biores.13.2.2887-2897
70. Richter AP, Brown JS, Bharti B et al (2015) An environmentally benign antimicrobial nanoparticle based on a silver-infused lignin core. Nat Nanotechnol 10:817–823. https://doi.org/10.1038/nnano.2015.141
71. Xiong F, Wu Y, Li G et al (2018) Transparent Nanocomposite Films of Lignin Nanospheres and Poly(vinyl alcohol) for UV-Absorbing. Ind Eng Chem Res 57:1207–1212. https://doi.org/10.1021/acs.iecr.7b04108
72. Liu X, Li C, Zhang D, Xiao Y (2006) Melting behaviors, crystallization kinetics, and spherulitic morphologies of poly(butylene succinate) and its copolyester modified with rosin maleopimaric acid anhydride. J Polym Sci Part B Polym Phys 44:900–913. https://doi.org/https://doi.org/10.1002/polb.20758
73. Joy J, Jose C, Yu X et al (2017) The influence of nanocellulosic fiber, extracted from Helicteres isora, on thermal, wetting and viscoelastic properties of poly(butylene succinate) composites. Cellulose 24:4313–4323. https://doi.org/10.1007/s10570-017-1439-y
74. Furushima Y, Schick C, Toda A (2018) Crystallization, recrystallization, and melting of polymer crystals on heating and cooling examined with fast scanning calorimetry. Polym Cryst 1:e10005. https://doi.org/https://doi.org/10.1002/pcr2.10005
75. Kovalcik A, Pérez-Camargo RA, Fürst C et al (2017) Nucleating efficiency and thermal stability of industrial non-purified lignins and ultrafine talc in poly(lactic acid) (PLA). Polym Degrad Stab

142:244–254. https://doi.org/https://doi.org/10.1016/j.polymdegradstab.2017.07.009

76. Weihua K, He Y, Asakawa N, Inoue Y (2004) Effect of lignin particles as a nucleating agent on crystallization of poly(3-hydroxybutyrate). J Appl Polym Sci 94:2466–2474. https://doi.org/https://doi.org/10.1002/app.21204
77. Kargarzadeh H, Galeski A, Pawlak A (2020) PBAT green composites: Effects of kraft lignin particles on the morphological, thermal, crystalline, macro and micromechanical properties. Polym (Guildf) 203:122748. https://doi.org/https://doi.org/10.1016/j.polymer.2020.122748
78. Bhat R, Abdullah N, Din RH, Tay G-S (2013) Producing novel sago starch based food packaging films by incorporating lignin isolated from oil palm black liquor waste. J Food Eng 119:707–713. https://doi.org/https://doi.org/10.1016/j.jfoodeng.2013.06.043
79. Michelin M, Marques AM, Pastrana LM et al (2020) Carboxymethyl cellulose-based films: Effect of organosolv lignin incorporation on physicochemical and antioxidant properties. J Food Eng 285:110107. https://doi.org/https://doi.org/10.1016/j.jfoodeng.2020.110107
80. Shikinaka K, Nakamura M, Navarro RR, Otsuka Y (2018) Plant-Based Antioxidant Nanoparticles without Biological Toxicity. ChemistryOpen 7:709–712. https://doi.org/https://doi.org/10.1002/open.201800157
81. Yang W, Fortunati E, Gao D et al (2018) Valorization of Acid Isolated High Yield Lignin Nanoparticles as Innovative Antioxidant/Antimicrobial Organic Materials. ACS Sustain Chem Eng 6:3502–3514. https://doi.org/10.1021/acssuschemeng.7b03782
82. Chen K, Qiu X, Yang D, Qian Y (2020) Amino acid-functionalized polyampholytes as natural broad-spectrum antimicrobial agents for high-efficient personal protection. Green Chem 22:6357–6371. https://doi.org/10.1039/D0GC01505A

Figures

Figure 1

Schematic illustration of S-LNPs preparation using anti-solvent precipitation assisted by ultrasonication.

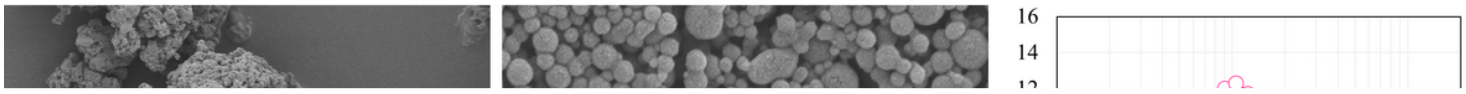

Figure 2

SEM micrograph of (a) S-lignin, (b) S-LNPs prepared from soluble-fraction fractionated from S-lignin and (c) particles size distribution of LNPs measured by Malvern Zetasizer-4.

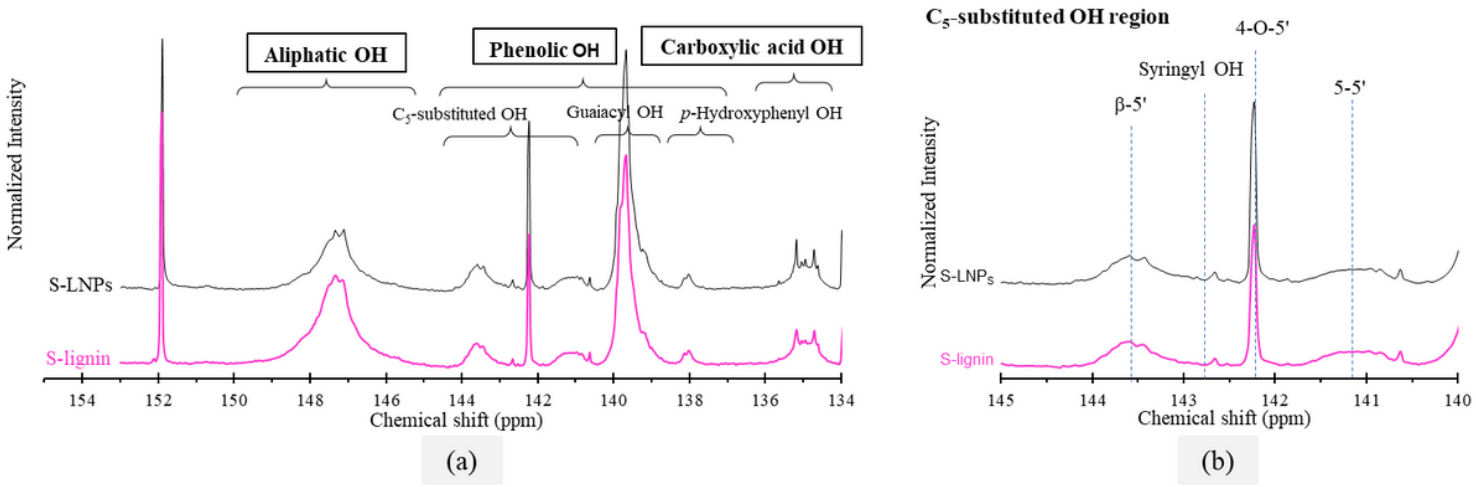

Figure 3

(a) ^{31}P NMR spectra of S-lignin and S-LNPs where aliphatic, phenolic and carboxylic hydroxyls are detected and (b) an enlarged view of C_5-substitutent hydroxyl region.

Figure 4

Photographs of (a) rolls of the neat PBS film and PBS/S-LNPs composite films, (b) single layer films to illustrate their transparency, and (c) optical micrographs of the neat PBS film and its composite films with either S-lignin or S-LNPs.

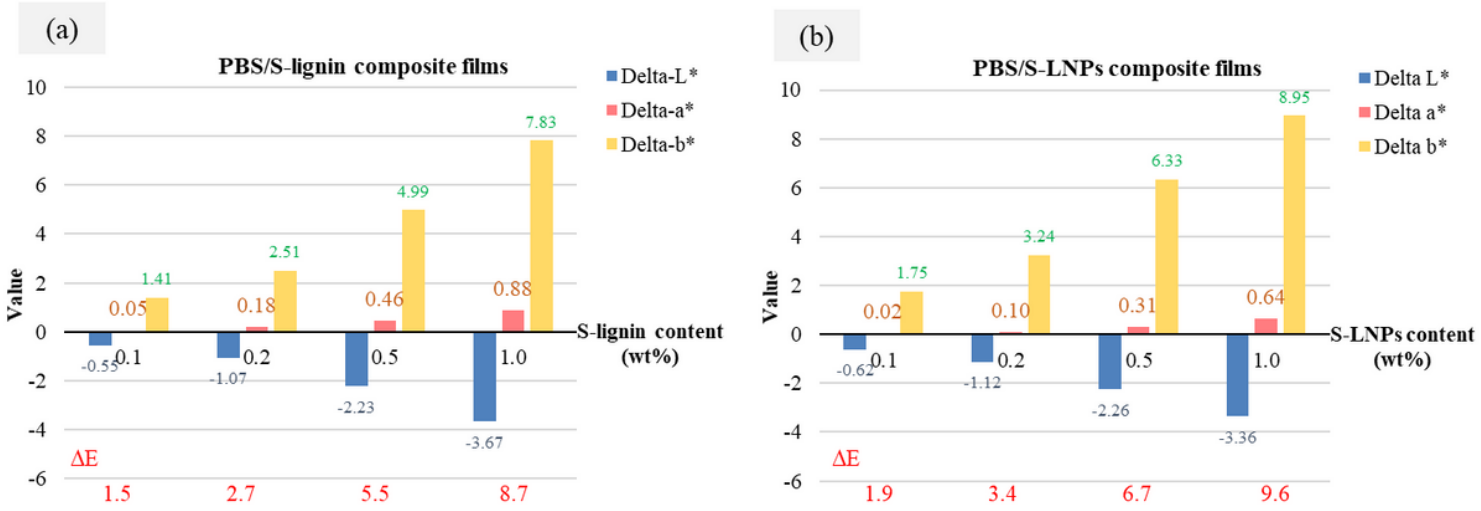

Figure 5

ΔL*, Δa* and Δb* results measured by colorimeter and calculated color difference (ΔE) of (a) PBS/S-lignin composite films and (b) PBS/S-LNPs composite films

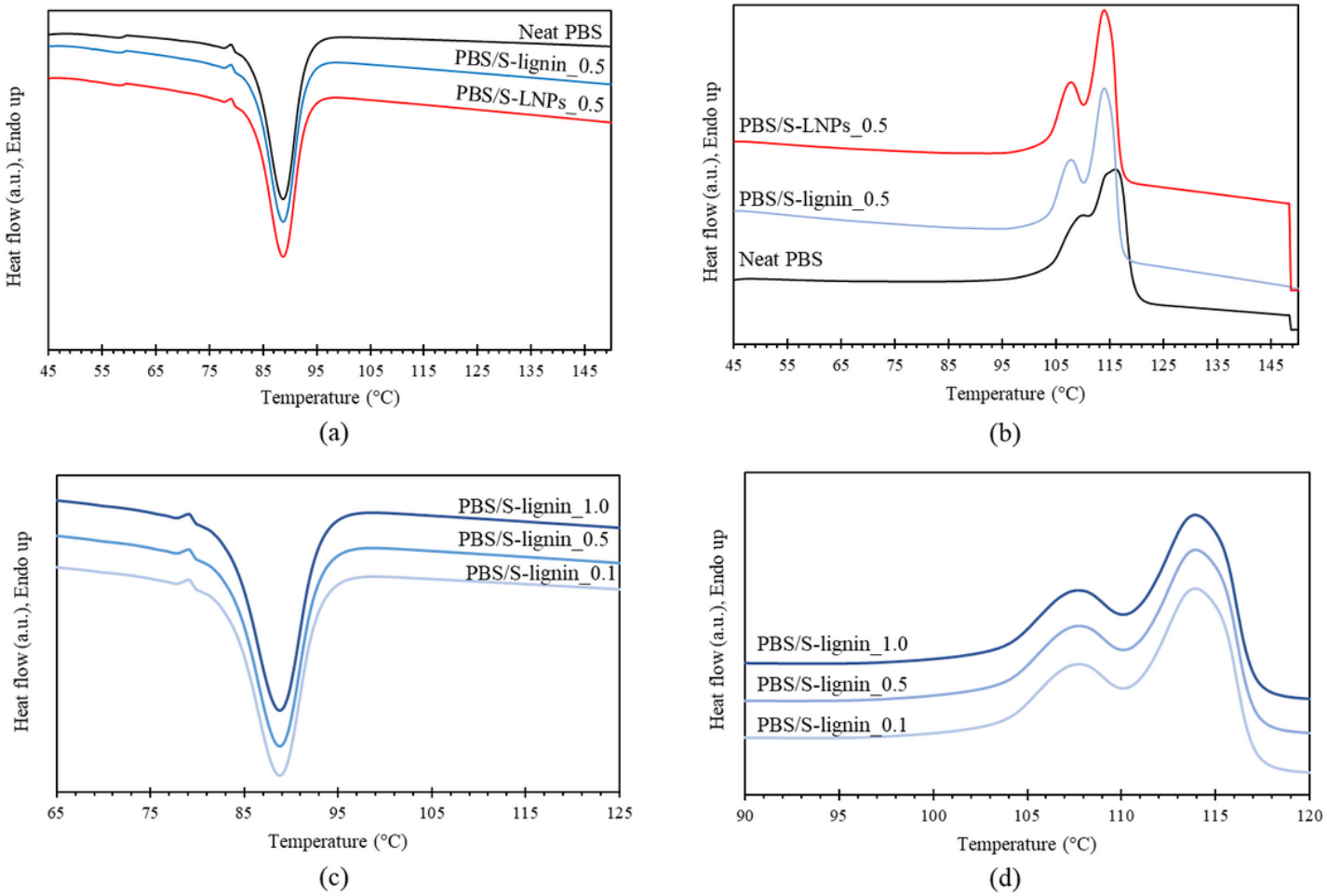

Figure 6

Overlaid DSC traces of neat PBS, PBS/S-lignin_0.5 and PBS/S-LNPs_0.5 films, traces obtained from (a) 1st cooling scan and (b) 2nd heat scan, (c) 1st cooling scan and (d) 2nd heat scan of PBS/S-LNPs composite films at different S-LNPs contents of 0.1, 0.5 and 1.0 wt%.

Figure 7

Overlaid of UV-vis spectra of the neat PBS film and its composite films; (a) PBS/S-lignin composite films, (b) PBS/S-LNPs composite films and (c) all PBS/S-lignin and PBS/S-LNPs composite films.

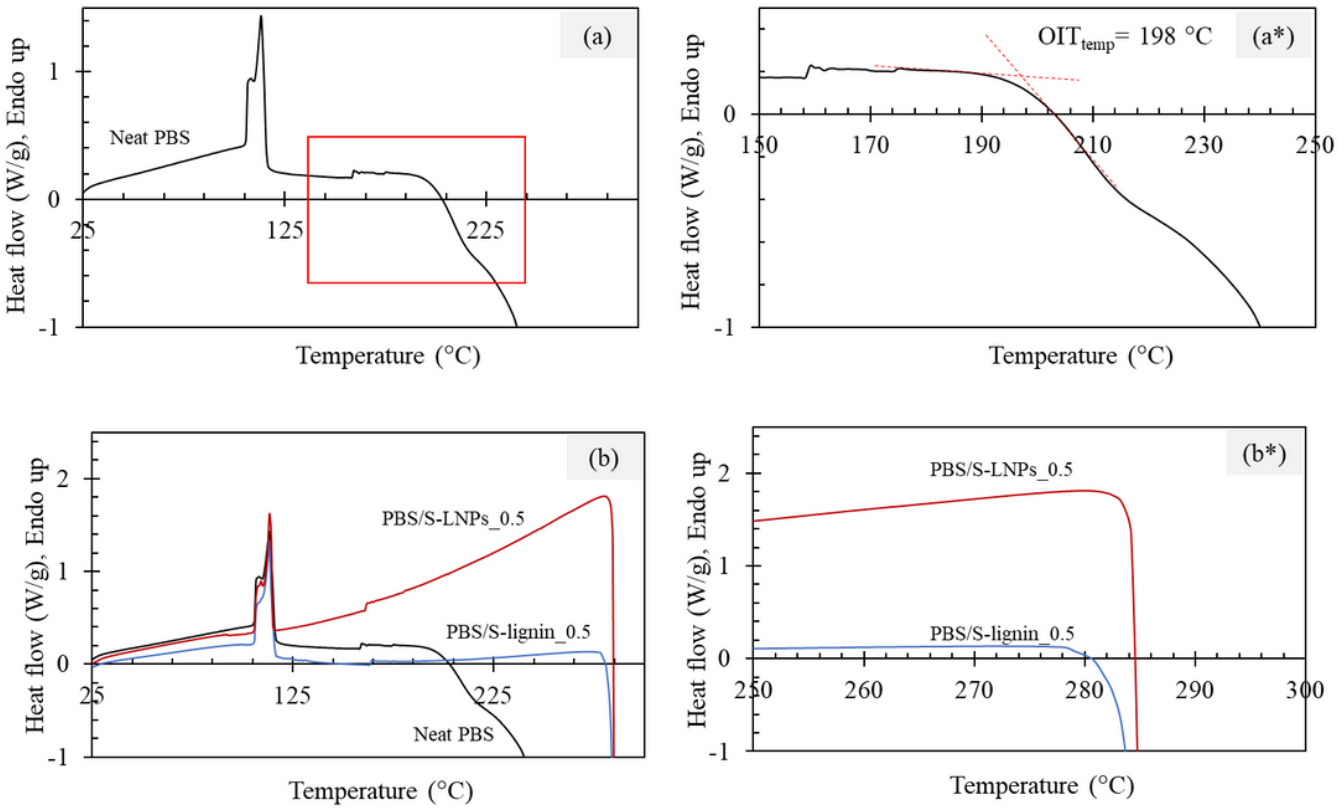

Figure 8

Oxidation induction temperature profiles of (a) the neat PBS, and (b) its composite films with 0.5 wt% S-lignin and S-LNPs.

Supplementary Files

This is a list of supplementary files associated with this preprint. Click to download.

- GraphicalAbstract.png